ACS APPLIED MATERIALS & INTERFACES

Research Article

www.acsami.org

Solvent Effects on the Structure–Property Relationship of Redox-Active Self-Assembled Nanoparticle–Polyelectrolyte–Surfactant Composite Thin Films: Implications for the Generation of Bioelectrocatalytic Signals in Enzyme-Containing Assemblies

M. Lorena Cortez,[†,‡] Marcelo Ceolín,[‡] Luis Cuellar Camacho,[§] Edwin Donath,[§] Sergio E. Moya,[∥] Fernando Battaglini,[*,†] and Omar Azzaroni[*,‡]

[†]INQUIMAE, Departamento de Química Inorgánica, Analítica y Química Física, Facultad de Ciencias Exactas y Naturales, Universidad de Buenos Aires, Ciudad Universitaria, Pabellón 2, C1428EHA, Buenos Aires, Argentina

[‡]Instituto de Investigaciones Fisicoquímicas Teóricas y Aplicadas (INIFTA), Departamento de Química, Facultad de Ciencias Exactas, Universidad Nacional de La Plata, CONICET, CC 16 Suc. 4 (1900), La Plata, Argentina

[§]Institute of Biophysics and Medical Physics, Faculty of Medicine, University of Leipzig, Leipzig, Germany

[∥]CIC biomaGUNE, Paseo Miramón 182, 20009 San Sebastián, Gipuzkoa, Spain

Supporting Information

ABSTRACT: The search for strategies to improve the performance of bioelectrochemical platforms based on supramolecular materials has received increasing attention within the materials science community, where the main objective is to develop low-cost and flexible routes using self-assembly as a key enabling process. Important contributions to the performance of such bioelectrochemical devices have been made based on the integration and supramolecular organization of redox-active polyelectrolyte–surfactant complexes on electrode supports. Here, we examine the influence of the processing solvent on the interplay between the supramolecular mesoorganization and the bioelectrochemical properties of redox-active self-assembled nanoparticle–polyelectrolyte–surfactant nanocomposite thin films. Our studies reveal that the solvent used in processing the supramolecular films and the presence of metal nanoparticles not only have a substantial influence in determining the mesoscale organization and morphological characteristics of the film but also have a strong influence on the efficiency and performance of the bioelectrochemical system. In particular, a higher bioelectrochemical response is observed when nanocomposite supramolecular films were cast from aqueous solutions. These observations seem to be associated with the fact that the use of aqueous solvents increases the hydrophilicity of the film, thus favoring the access of glucose, particularly at low concentrations. We believe that these results improve our current understanding of supramolecular nanocomposite materials generated via polyelectrolyte–surfactant complexes, in order to use the processing conditions as a variable to improve the performance of bioelectrochemical devices.

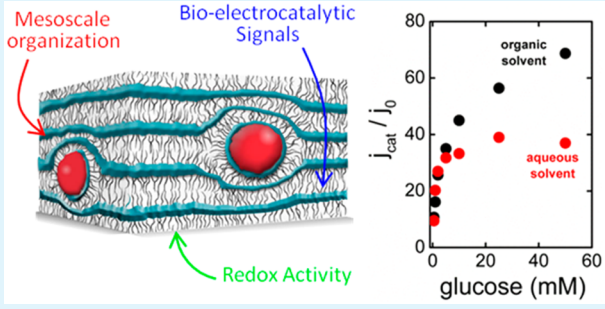

KEYWORDS: *bioelectrochemistry, structure–property relationship, nanocomposite thin films, polyelectrolyte–surfactant complexes, redox-active polymers, metal nanoparticles, self-assembly, supramolecular materials*

1. INTRODUCTION

The conversion of chemical reactions into an electrical current is the focus of intense research in materials science because of their potential applications in solar energy conversion, fuel cells, and sensors, among others.[1−6] To achieve this goal, a surface should be properly modified in order to produce an efficient electron-transfer process from the phase containing the reactants to the electrical conductor. In the case of fuel cells and amperometric sensors, this interphase is represented by the electrode surface and its modification through different strategies is used for the generation of different architectures to meet different requirements, such as improving the reduction of oxygen[7] and the methanol oxidation[8] or allowing electron-transfer processes with redox proteins.[9] Several redox enzymes have an important role either in biosensors (i.e., oxidases, dehydrogenases) or in biofuel cells (multicopper oxidases), and they require an adequate interfacial environment to accomplish an efficient electron-transfer process.[10−12]

In particular, electrode materials with a high surface/volume ratio can increase the amount of immobilized enzyme on the

Received: October 21, 2016
Accepted: December 15, 2016
Published: December 15, 2016

DOI: 10.1021/acsami.6b13456
ACS Appl. Mater. Interfaces 2017, 9, 1119−1128

electrode, minimize the mass-transport barriers for the substrate, and generate a chemically and mechanically robust system. The use of nanocomposites integrating metallic nanoparticles has demonstrated a promising potential to improve the redox connectivity between the bioactive elements and the electrode surface.[13,14] It is also important to note that these nanocomposites should not interfere with the biological activity of the enzyme; otherwise, the sensitivity and selectivity of the sensor might be compromised. Gold nanoparticles (AuNPs) have been more widely explored and successfully implemented in the construction of three-dimensional interfaces with improved sensitivity and biorecognition properties.[15,16] The large surface/volume ratio of nanoparticles with their single optical/electronic properties has encouraged their increased application in this field.[17−20] In particular, AuNPs have a strong adsorption capacity and high catalytic efficiency; they are used as electron-transfer mediators to amplify the rate of electron transfer between enzymes and electrodes.[21,22]

On the other hand, in recent years, the interest in supramolecular materials based on polyelectrolyte−surfactant complexes shifted toward electrochemical applications.[23−29] The complexation of ionic surfactants with oppositely charged polyelectrolytes has opened a pathway toward the molecular design of functional materials, and, consequently, because of possible versatile variations of the two counterparts, a wealth of supramolecular assemblies can be created.[30−34] In this context, in previous reports we presented the construction of self-assembled structures onto different surfaces from the casting of an organic solution containing redox-active polyelectrolyte and sodium dodecyl sulfate employing a one-step deposition process, either by drop casting or spin coating, followed by solvent evaporation.[35] In addition, we have shown the capabilities of these films to adsorb an enzyme and work as amperometric sensors.[36−38] This simple strategy allowed us to decrease the preparation time, compared to organized systems constructed by layer-by-layer processes,[39−42] and avoid the use of cross-linking reagents that can affect the enzyme activity.[43,44] More recently, this approach enabled us to create mesostructured polyelectrolyte−surfactant nanoarchitectures efficiently by integrating glucose oxidase onto gold electrodes using aqueous solvents for the casting process. These enzyme-containing mesoorganized supramolecular assemblies exhibited interesting changes in their mesostructure when they were exposed to a humid environment and displayed a more effective response at low glucose concentrations.[45]

Regarding this issue, it is important to consider that the formation of self-assembled supramolecular structures from solution onto solid supports is highly dependent on a number of weak forces that can lead to particular mesoscale patterns under a range of chemical and environmental conditions, including the type of solvent.[46−48] Despite intensive research exploring the correlation between the supramolecular structure, film morphology, and functional properties, to date, it is still not known how the processing solvent impacts the mesostructural and charge-transport characteristics of redox-active polyelectrolyte−surfactant composite films. Therefore, a detailed investigation of the processing-solvent-dependent supramolecular organization and charge-transport properties can significantly enhance the understanding of several functional features of these types of supramolecular materials. In addition, research on improving the processing solvents of such films is necessary to replace good film forming but toxic solvents such as chloroform and toluene. Therefore, the ability to process polyelectrolyte−surfactant composite films from environmentally benign solvents such as water can make them much stronger candidates for industrial bioelectrochemical applications at a lower cost. Taking into account these concepts and being aware of the critical role played by the self-assembly solvent and the presence of metal nanoparticles in the functional properties of the redox-active nanocomposites, we focused our research efforts on analyzing the implications and influence of these two factors on the generation of bioelectrocatalytic signals in enzyme-containing assemblies. One of the key outcomes from our studies is a demonstration that the solvents used in processing the supramolecular films and the presence of metal nanoparticles have a substantial influence in determining the mesoscale organization, the morphological characteristics in the presence of aqueous environments, and the efficacy of charge and solute transport in the bioelectrochemical system. We believe that our studies contribute to improving the current understanding of the structure−property relationships in polyelectrolyte−surfactant complexes, which may pave the way toward improving design strategies of nanocomposite supramolecular materials with optimized electrochemical functions.

2. EXPERIMENTAL SECTION

2.1. Reagents and Materials. Sodium dodecyl sulfate (SDS) and glucose oxidase (GOx) were purchased from Sigma-Aldrich, and tris(hydroxymethyl)aminomethane, D-(+)-glucose, and dimethylformamide (DMF) were obtained from Carlo Erba. The redox polymer $Os(bpy)_2ClpyNHpoly(allylamine)$ (OsPA) was synthesized as previously reported.[49] The stoichiometry ratio between the osmium complex and the allylamine monomer was 1:35. AuNPs with a diameter of 11 ± 3 nm were synthesized according to a reported procedure.[50] All other reagents were of analytical grade.

A glucose solution was prepared in a Tris−HCl buffer (pH 7.4) and left at 4 °C overnight to allow equilibration of the anomers.

2.2. Preparation of the Polyelectrolyte−Surfactant Composite Material (OsPA−DS). A total of 200 μL of SDS (10 mM) in Milli-Q water was added to 100 μL of OsPA (0.2 mM) in Milli-Q water. The mixture generated a precipitate (OsPA−DS), which was easily separated by centrifugation. The precipitate was dissolved in 250 μL of DMF and sonicated for 15 min to facilitate complete dissolution of the solid.

2.3. Preparation of Polyelectrolyte−Surfactant−AuNP Composite Materials (OsPA−DS−AuNP). *a. Polyelectrolyte−Surfactant−AuNP Composite Material from an Organic Solution [OsPA−DS−AuNP(o)].* A 2 mL AuNP suspension was centrifuged at 3600 rpm for 60 min. The resulting pellet was resuspended with 50 μL of DMF and sonicated for 30 min to obtain a well-dispersed suspension. A total of 100 μL of the DMF solution of OsPA−DS previously described was then added to the AuNP suspension and sonicated for 30 min to give a homogeneous dispersion. The final dispersion was used for substrate modification.

b. Synthesis of the Polyelectrolyte−Surfactant−AuNP Composite Material from an Aqueous Solution [OsPA−DS−AuNP(a)]. A 2 mL AuNP suspension was centrifuged at 3600 rpm for 60 min. The resulting pellet was resuspended with 100 μL of SDS (10 mM) and sonicated for 30 min to obtain a well-dispersed suspension. This suspension was mixed with 50 μL of OsPA (0.2 mM). The precipitate was discarded, and the final dispersion was used for substrate modification.

2.4. Substrate Modification. Gold was used as the substrate in the electrochemical experiments, and in all of the other experiments, the substrate was silicon. Substrates were modified by the same experimental procedure. The first step consisted of the application by spin coating of a thin layer of the corresponding solution. Afterward, the substrates were left at room temperature for 4 h to allow complete

DOI: 10.1021/acsami.6b13456
ACS Appl. Mater. Interfaces 2017, 9, 1119−1128

Scheme 1. Illustrative Schematic Depicting (a) the Constituting Building Blocks Participating in the Generation of the Supramolecular Material, (b) the Formation of Mesoscale-Organized Polyion−Surfactant Complexes, (c), the Formation of Films via Drop Casting on Solid Substrates Using Aqueous or Organic Solvents, and (d) the Configuration of the Outermost Layer Leading to Supramolecular Films with Hydrophilic or Hydrophobic Character

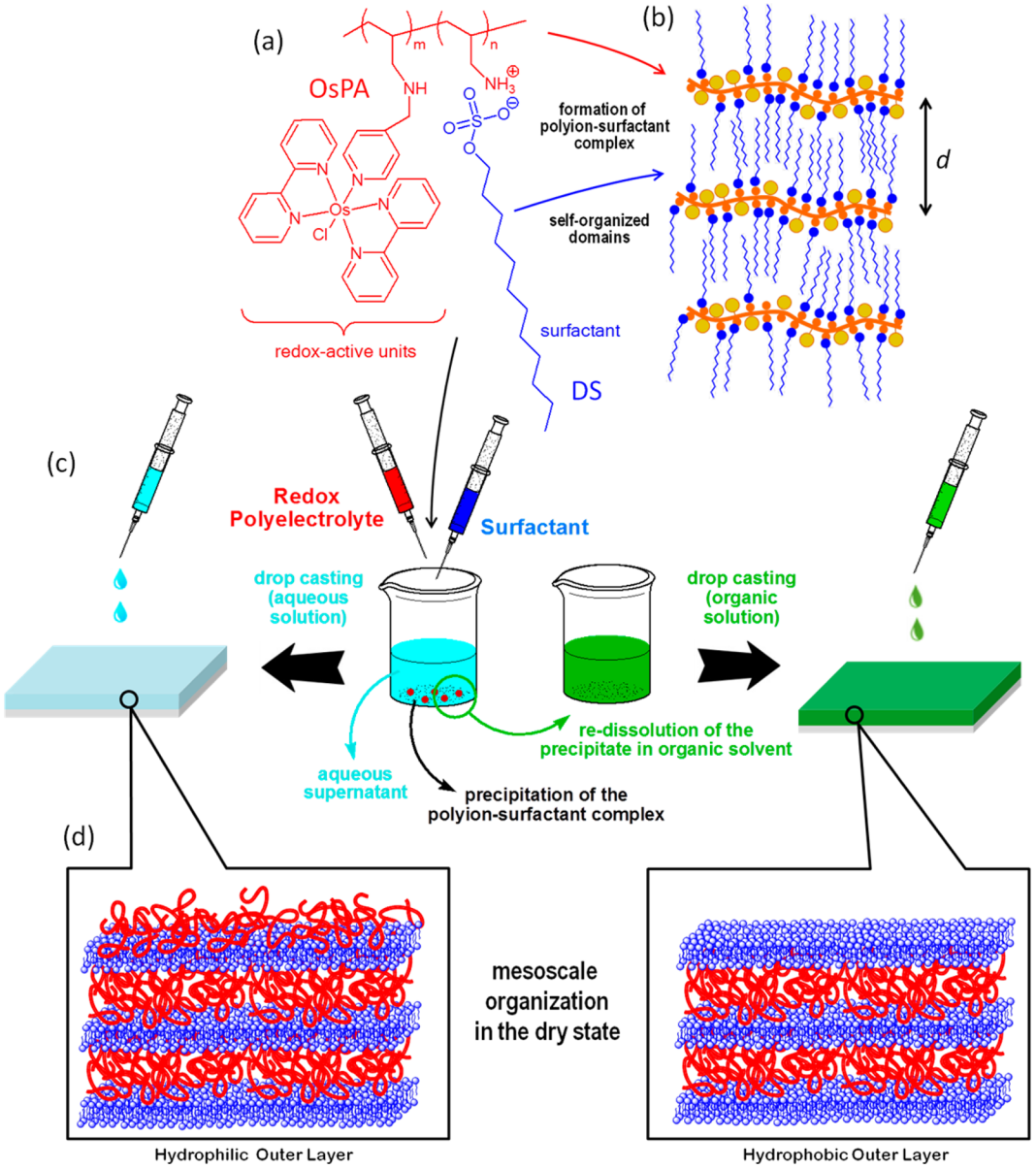

evaporation of the solvent. Then, they were rinsed with Milli-Q water and dried under a stream of nitrogen gas.

2.5. Equipment. *Spin Coating.* Thin polymer films were prepared by spin coating using a commercial spin coater (Laurell WS-400B).

Electrochemical Measurements. Films were cast onto gold sputtered on silicon wafers by spin coating, as was previously explained. GOx adsorption was carried out by immersion of the films in a 1 mg mL^{-1} GOx solution in 0.1 M Tris buffer (pH 7.4) and 0.1 M NaCl for 1 h.

Cyclic voltammetry experiments were carried out using a Teq-02 potentiostat (TEQ, Argentina) with a three-electrode Teflon electrochemical cell equipped with a platinum mesh counter electrode and an Ag/AgCl reference electrode. Unless otherwise stated, all electrochemical experiments were performed at room temperature (22 °C) in a 0.1 M Tris−HCl and 0.1 M NaCl buffer solution at pH 7.4. Studies of the electrochemical response of the films were carried out after the films yielded a constant cyclic voltammetry response.

Contact-Angle Measurements. A KSV Cam200 equipment was used for contact-angle measurements. Distilled water was used as a liquid probe in all assays.

Grazing-Incidence Small-Angle X-ray Scattering (GISAXS). GISAXS measurements were performed at the D10AXRD2 beamline of the Laboratório Nacional de Luz Síncrotron (LNLS, Campinas, Brazil; λ = 1.608 Å). The sample-to-detector distance was kept at 550 mm, and the outgoing photons were detected using a PILATUS 100 K detector (DECTRIS AG, Baden-Daettwil, Switzerland). The sample temperature was kept to 20 °C, and the sample humidity was controlled using a home-built chamber.

Atomic Force Microscopy (AFM). To monitor changes in the surface topography, AFM imaging was performed using a Molecular Force Probe 3D (Asylum Research, Goleta, CA) in contact mode. Soft cantilevers (0.02 N m^{-1}) with sharp silicon nitride tips (Si_3N_4 tip radii < 20 nm) were used throughout all measurements. Before the experiment was run, the deflection sensitivity was obtained from a force−distance curve performed on a hard glass surface. Afterward, the

DOI: 10.1021/acsami.6b13456
ACS Appl. Mater. Interfaces 2017, 9, 1119−1128

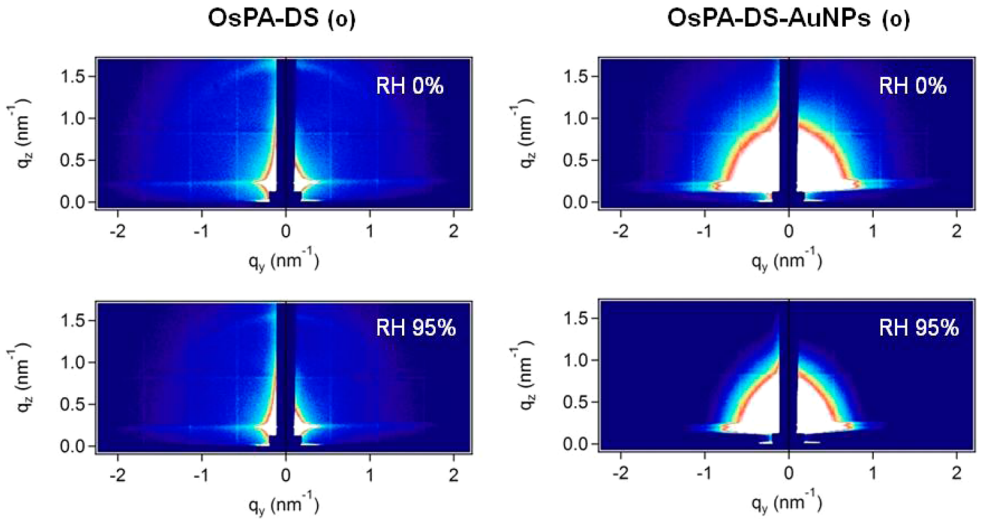

Figure 1. GISAXS patterns obtained from (left) OsPA–DS(o) and (right) OsPA–DS–AuNP(o) films measured at an incident angle of 0.27° under low-humidity (top) and high-humidity (bottom) conditions. Films were cast onto Si(100) substrates.

thermal noise method was used to determine the spring constant of the cantilever.[51] Each sample was first imaged in the dry state and then in liquid conditions and at room temperature. First, large surface areas of about 20 μm were scanned to acquire a broad overview of the surface topography; subsequently, smaller regions of 5 μm were imaged to identify characteristic features on the surface in more detail. Scan rates of 0.3–0.8 Hz were applied during imaging, and a minimal loading force between the tip and the sample surface was always maintained by decreasing the set-point value to the point just above where the tip started to lose its contact with the surface. This has been done in order to minimize possible damage induced by the tip to the surface due to shear forces.

The roughness of the surface was obtained with the *IGOR Pro* software, which calculates the root-mean-square (rms) deviation of the surface morphology through

$$R_s = \sqrt{\frac{1}{MN}\sum_{j}^{M}\sum_{i}^{N}\eta^2(xy_j)^2}$$

where M is the number of points per scan line, N is the number of taken profiles within an area, and η is the amplitude at a particular x–y position.

3. RESULTS AND DISCUSSION

Polyelectrolyte–surfactant complexes have been previously used to functionalize different electrode surfaces (graphite, gold, indium–tin oxide, etc.). In all of these cases, the complexes were used either as a colloidal suspension in water[19] or as an organic solution in DMF,[20−22] closely resembling the seminal works of Thünemann et al.[52−54] In particular, when the polyelectrolyte is modified with a polypyrridylosmium complex, the mixture with SDS produces a precipitate that can be separated from the supernatant and redissolved in DMF. If the SDS concentration in the mixture is reduced, we found that only a small amount of complex precipitates, with both species thus remaining in solution (Scheme 1). Again, the precipitate can be separated and redissolved in DMF; in this way, two precursors are obtained for the generation of an electroactive film (Scheme 1). Then, AuNPs can be suspended in the precursor solutions, yielding a stable suspension. Thermogravimetric analysis (TGA) revealed that, on average, the polymer–metal nanoparticle composition in the obtained nanocomposite film is close to 60:40. Concomitantly, X-ray photoelectron spectroscopy (XPS) confirmed the presence of polyelectrolyte–surfactant complexes with a ratio close to 1:1 between the allylamine monomer and dodecyl sulfate (N:S ratio) as well as the presence of gold in the nanocomposite films (see the Supporting Information for details). These suspensions were cast onto silica and gold to study its structure, ability to incorporate GOx, and electrochemical response. The results are compared with those from films formed without AuNPs.

GISAXS studies were carried out to characterize the structures of the films and the changes that the incorporation of AuNPs can eventually produce. In Figure 1, GISAXS patterns for films cast from organic solutions with OsPA–DS–AuNP(o) and without AuNPs [OsPA–DS(o)] measured under different humidity conditions are shown. As was observed in previous works,[21] the organic system without AuNPs (Figure 1) shows bright spots in the q_z direction, suggesting that the film is mesoorganized, forming lamellar domains oriented parallel to the substrate. The lamellar structure could be represented by alternating layers of hydrophobic alkyl tails and hydrophilic domains of the OsPA polyelectrolyte with a lamellar spacing of 3.78 nm, as measured by GISAXS. It is well-known that water uptake may lead to the swelling of hydrophilic polyelectrolyte domains in phase-segregated materials.[55] Considering that aqueous environments represent a more realistic scenario for the study of the function–structure properties of these systems, we assessed the influence of water on the mesoscale organization of these systems. To this end, we performed GISAXS experiments under high humidity conditions, i.e., reaching saturation. We observed that exposure to a very humid environment (relative humidity ∼95%; Figure 1) induces a shift in the position of the halo, indicating a slight swelling of the lamellar mesostructure due to the presence of water. GISAXS measurements revealed that the lamellar spacing of OsPA–DS(o) films changed from 3.78 to 4.11 nm due to the swelling of hydrophilic domains. On the other hand, in the case of films cast from organic solutions containing AuNPs, the GISAXS patterns measured in dry and humid conditions are dominated by the nanoparticle scattering, preventing a detailed film structure analysis; however, we can univocally identify two relevant features: (a) the presence of AuNPs in the film due to the strong scattering and (b) the absence of mesoorganization, as observed in nanoparticle-free

DOI: 10.1021/acsami.6b13456
ACS Appl. Mater. Interfaces 2017, 9, 1119–1128

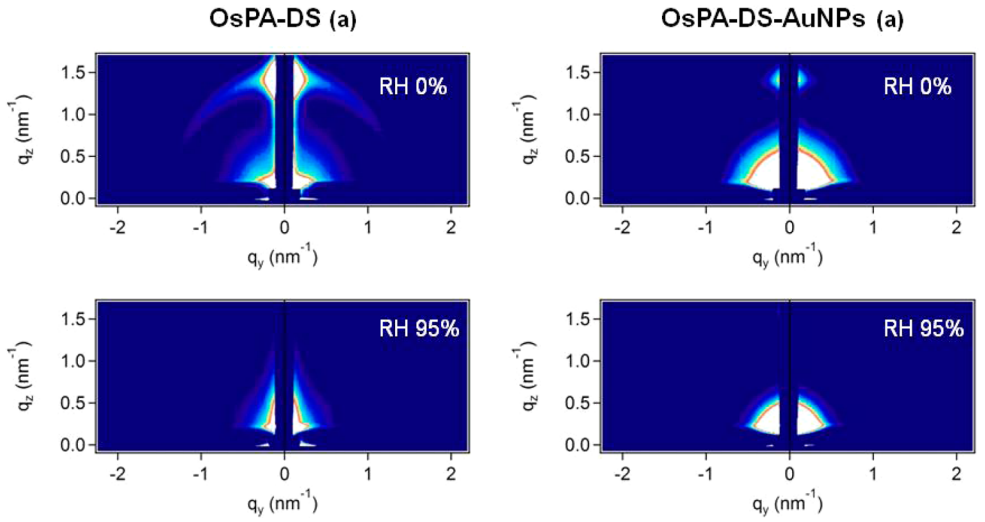

Figure 2. GISAXS patterns obtained from (left) OsPA–DS(a) and (right) OsPA–DS–AuNP(a) films measured at an incident angle of 0.27° under low-humidity (top) and high-humidity (bottom) conditions. Films were cast onto Si(100) substrates.

films, due to the absence of bright spots or halos in the GISAXS pattern. These experimental observations indicate that the presence of AuNPs promotes significant changes in the film structure, precluding the formation of lamellar domains when films are cast from organic solutions.

Conversely, in the case of films cast from aqueous solutions, GISAXS patterns measured in the "dry" state reveal that films prepared in the presence and absence of nanoparticles present a well-defined lamellar order. This is evident by the presence of halos or bright spots (Figure 2). Films prepared in the absence of AuNPs exhibit a bright region (highest intensity) in the direction q_z (for $q_y \rightarrow 0$) and the presence of a faint halo. This suggests the presence of lamellar domains mostly oriented parallel to the substrate with a lamellar spacing of 4.24 nm. It is worth noting that the faint-halo GISAXS pattern might also indicate that a fraction of these domains are multioriented. Then again, films cast from aqueous solutions containing AuNPs exhibit a very bright spot in the direction q_z, but the absence of a faint halo indicates that these films in the "dry" state can be presented by a well-ordered lamellar mesoorganization oriented parallel to the substrate with a lamellar spacing of 4.13 nm. This experimental fact illustrates the critical role played by the solvent during the self-assembly and mesoorganization of the nanocomposite. However, such mesoorganization is vanished when both films (with and without AuNPs) are exposed to a humid environment (Figure 2), and it cannot be recovered when the system is back to dry conditions, thus showing an important difference with respect to that observed in organic systems.

From these observations, it can be concluded that the use of an aqueous medium in the construction of these types of films promotes drastic changes not only in the film mesostructure but also in the film reorganization upon exposure to water. Contrary to that observed in films prepared in organic solvents, the presence of water in the self-assembly process leads to the formation of mesoscale-organized "dry" films that lose organization in the presence of water.

To shed light on the interaction of both types of films with water, we carried out contact-angle measurements on films cast from organic solvents and aqueous solutions and in the absence and presence of AuNPs. The results are depicted in Table 1, showing that the processing solvent has a strong impact on the

Table 1. Contact-Angle Measurements

sample	contact angle (deg)	sample	contact angle (deg)
OsPA–DS(o)	90	OsPA–DS(a)	49
OsPA–DS–AuNP(o)	92	OsPA–DS–AuNP(a)	52

affinity of the film for water. The hydrophobic behavior exhibited by films processed from organic solutions can be attributed to organization of the outermost layers exposing aliphatic moieties to the solution.[56] On the other hand, the lower value in the contact angle for the films processed from aqueous solutions suggests that the outer layer exposed hydrophilic groups to the solution. Also, the fact that the hydrophilic moieties (amino and sulfate groups) are able to retain water molecules has to be considered, thus further increasing the hydrophilic character of the film.[57] In these conditions, the film resembles a self-assembled layer-by-layer system where contact angles range between 30 and 60°.[58] The experiments further confirm that the processing solvent preconfigures the affinity and type of interaction of the nanocomposite with the aqueous environment, i.e., hydrophobic versus hydrophilic interactions.

In addition, it is plausible to assume that the influence of the processing solvent on the mesoscale organization and affinity to water might also have an impact on the morphological characteristics of the cast films. To confirm this assumption, AFM characterization of the systems was performed. First, the samples were analyzed in ambient conditions, i.e., in air, to characterize the surface morphology of the film in the "dry" state. Next, the films were exposed to a buffer solution, always using the minimum contact normal force between the tip and sample to minimize the distortion applied to the film. The AFM results are shown in Figure 3.

In the case of "dry" organic systems, a rather compact and rough structure exhibiting some protrusions of 30–50 nm in height (Figure 3) can be observed. However, when the film was exposed to the buffer solution, a significant reorganization of the film was observed. These morphological changes involved the enlargement of the protrusions, which in some regions were 200 nm in depth. This morphological reorganization was

DOI: 10.1021/acsami.6b13456
ACS Appl. Mater. Interfaces 2017, 9, 1119–1128

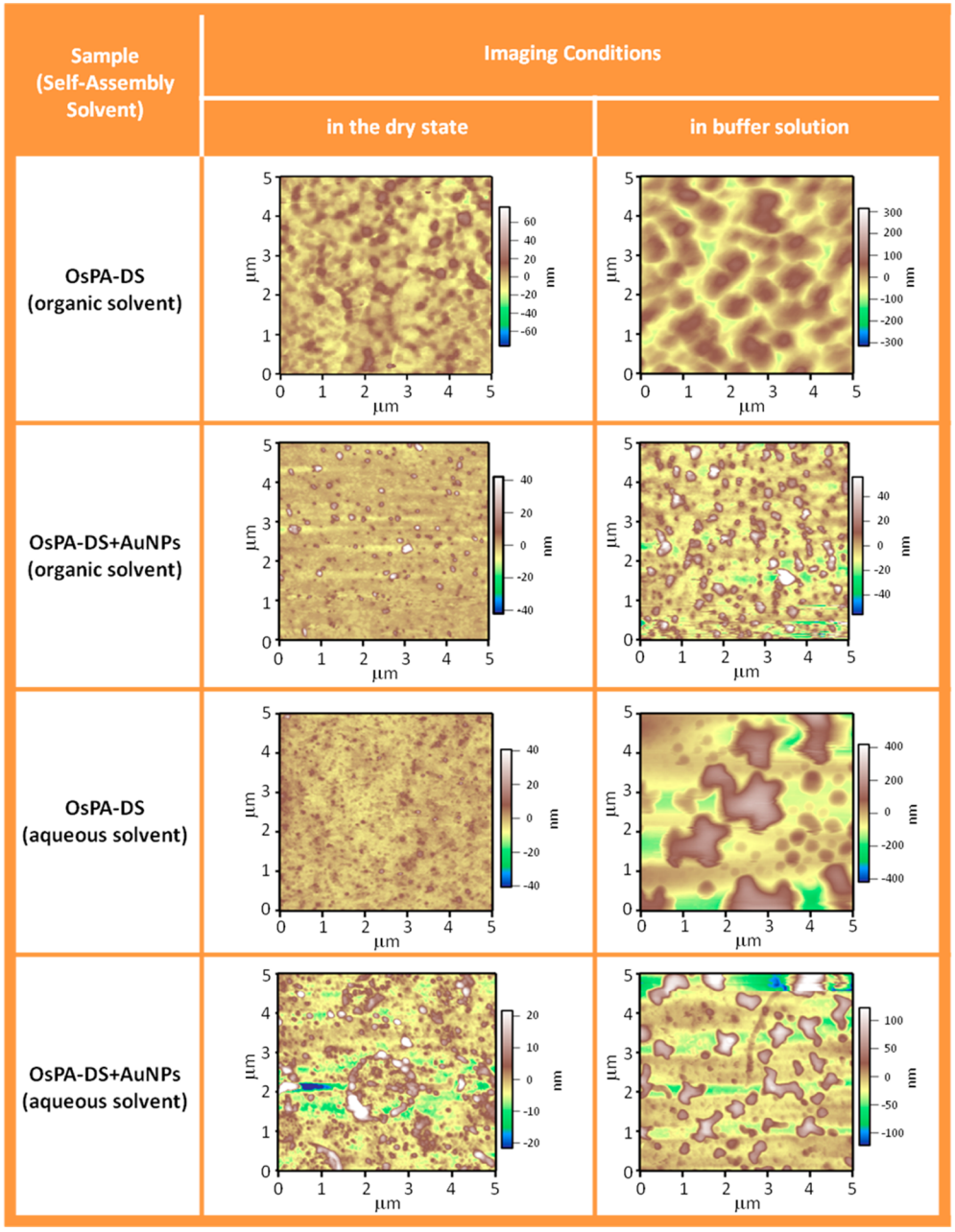

Figure 3. Topographic AFM images corresponding to OsPA–DS assemblies and OsPA–DS–AuNP nanocomposite thin films cast from aqueous and organic solutions measured under different experimental conditions: (left) in air (dry state); (right) in a buffer solution.

quantified by measuring the film roughness (as derived from the rms deviation of the surface morphology R_{rms}; see the Experimental Section). These values are depicted in Table 2.

Films cast from organic solutions containing AuNPs (Figure 3) exhibited a compact and smooth morphology as well as the presence of small protrusions in their topography. These protrusions are 30–50 nm and could be attributed, to some extent, to the presence of AuNPs on the film surface. Introducing the sample in the buffer solution also involved morphological changes; however, these topographical changes were less significant than those observed in films without AuNPs (see Table 2). This fact reinforces the idea that the polyelectrolyte–surfactant system strongly interacts with the nanoparticles, resulting in a more stable and rigid structure.

In the case of films cast from aqueous solutions, the structural changes observed when passing from the "dry" state to the buffer solution are more striking. This observation is in close agreement with the GISAXS results. The dry film without AuNPs showed a rather granular and compact structure that, after exposure to a buffer solution, underwent a major morphological transition, yielding large aggregates and protrusions across the surface. For the sake of comparison, it

Table 2. rms Roughness of the Investigated Samples

	R_{rms} (nm)			
	OsPA–DS(o)	OsPA–DS–AuNP(o)	OsPA–DS(a)	OsPA–DS–AuNP(a)
dry state	8 ± 2	4 ± 2	3 ± 1	7 ± 2
in a buffer	38 ± 5	14 ± 4	92 ± 4	38 ± 5

DOI: 10.1021/acsami.6b13456
ACS Appl. Mater. Interfaces 2017, 9, 1119–1128

is worth adding that the roughness increases upon exposure to a buffer 3 times higher than that measured in films cast from organic solvents. The film containing AuNPs in dry conditions showed a high density of small protrusions, similar to the AuNP system cast from an organic solvent. When these films were exposed to a buffer solution, AFM imaging revealed the presence of protrusions (150 nm in height) and R_{rms} values of 38.3 nm. Even though there is an increase in the roughness after exposure to the buffer solution, it is important to note that the roughness increase in AuNP-containing films is much smaller than that observed in nanoparticle-free films (6 vs 31 times; see Table 2). This demonstrates that also in the case of films cast from aqueous solutions the presence of AuNPs has a strong impact on the structural reorganization of the supramolecular nanocomposite thin film. We should also note that we have used phase imaging as a real-time contrast enhancement technique. Phase imaging is a versatile extension of tapping-mode AFM that provides nanometer-scale information about the surface structure and can detect variations in the composition. In our case, we have observed that phase imaging of OsPA–DS films was featureless; however, similar experiments performed on OsPA–DS–AuNP nanocomposites revealed the presence of evenly distributed nanoparticles in the polymer film (see the Supporting Information for details).

Once the effect of the processing solvent and AuNPs on the morphological and structural characteristics of the nanocomposite films had been examined, we proceeded to study the influence of these variables on the functional properties of the obtained interfacial architectures. The four types of films described above were cast onto gold electrodes by spin coating and modified with GOx by adsorption (see the Experimental Section). The average surface coverage of GOx on the nanocomposite thin films was 2.8 μg cm^{-2}, as determined by microgravimetric measurements (see the Supporting Information for details). These modified electrodes were immersed in a buffer solution, and the potential was cycled until a stable response was observed. To evaluate the performance of each type of film, the peak current density obtained at 10 mV s^{-1} was used as a reference in further experiments (j_0). In all cases, the addition of glucose produces a well-defined catalytic current that increases as the concentration of glucose increases. As an example, Figure 4 shows the response observed for a gold electrode modified with a film containing AuNPs cast from an aqueous solution.

In order to compare the effect of the solvent and the presence of nanoparticles, the catalytic current density (j_{cat}) was normalized by j_0 because the coverage is not the same in all cases. Figure 5 depicts the ratio j_{cat}/j_0 plotted versus glucose concentration for electrodes modified by casting organic and aqueous solutions in the presence and absence of AuNPs. Voltammetric data reveal two important effects; one produced by the solvent and the other produced by the presence of AuNPs. Films cast from aqueous solutions exhibit a sharper slope at low glucose concentrations and reach the maximum signal at 25 mM; meanwhile, those electrodes cast from organic solvents reach the maximum signal at 50 mM. The other effect can be attributed to the presence of AuNPs in the nanocomposite film. It can be observed that in both cases (aqueous and organic solvent processing) the addition of AuNPs sharply increases the catalytic response of the film, being more prominent in the case of films cast from organic solvents. As revealed by phase imaging by AFM (see Figure S4 in the Supporting Information), their introduction generates a

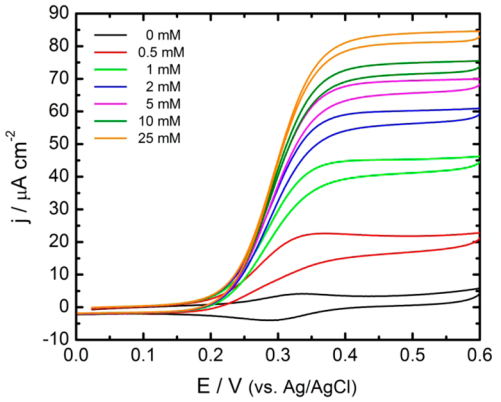

Figure 4. Bioelectrocatalytic response (current vs applied potential) of a OsPA–DS–AuNP(aq)/GOx-modified electrode in the presence of increasing amounts of glucose. Electrolyte: 100 mM Tris–HCl buffer (pH 7.4) + 0.1 M NaCl.

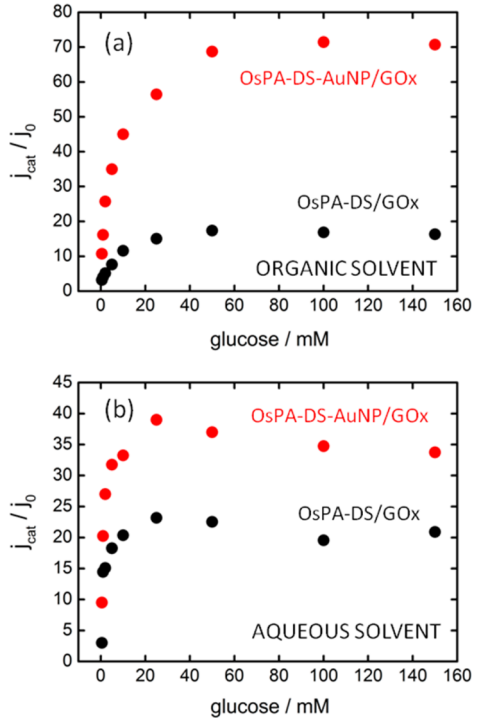

Figure 5. Representation of the j_{cat}/j_0 ratio as a function of the glucose concentration (j_{cat} = current density observed in the presence of glucose and j_0 = current density observed in the absence of glucose). Panel a depicts the bioelectrocatalytic response of electrodes modified with OsPA–DS–AuNP/GOx nanocomposites (red circles) and OsPA–DS/GOx assemblies (black squares) cast from organic solutions. Panel b depicts the bioelectrocatalytic response of electrodes modified with OsPA–DS–AuNP/GOx nanocomposites (red circles) and OsPA-DS/GOx assemblies (black squares) cast from aqueous solutions.

film with evenly distributed nanoparticles in the polymer film. This fact, combined with previous observations (ref 38) showing that AuNPs improve electron transfer among osmium centers and that GOx is predominantly adsorbed onto the AuNPs rather than the polymeric domains, leads us to propose that the overall effect relies on the close interaction between the enzymes and the redox centers, thus improving the electron-transfer rate in the film and, in turn, the bioelectrocatalytic

DOI: 10.1021/acsami.6b13456
ACS Appl. Mater. Interfaces 2017, 9, 1119–1128

current. The order in the bioelectrocatalytic current response is OsPA−DS−AuNP(o) > OsPA−DS−AuNP(a) > OsPA−DS(a) > OsPA−DS(o), and it can be rationalizedby taking into account the three factors required for an efficient oxidation of glucose on a modified electrode. One of them is related to the random distribution of the osmium centers in the film to facilitate the electron-transfer process to the electrode. The other two factors are related to the chemical reaction: facile access of glucose molecules to the film and close interaction between the enzyme and the osmium centers. The use of an aqueous solvent facilitates the access of glucose, particularly at low concentrations, because the film is more hydrophilic. On the other hand, the presence of AuNPs not only helps to maintain the structural stability of the films but also facilitates the "wiring" of the enzyme and the redox polyelectrolyte because they act as metal nanoelectrodes dispersed in the nanocomposite matrix. Also note that, according to GISAXS experiments, the presence of AuNPs has a disruptive effect on the mesoscale organization and lamellar stratification of the film, and this, in turn, facilitates the random distribution of the redox centers. From the results presented here, we can confirm that the use of AuNPs and organic solvents for processing the supramolecular nanocomposite produces rather compact interfacial architectures displaying no mesostructural organization or even short-range lamellar stratification. From the data plotted in Figure 5, it is clear that those films containing AuNPs exhibit a better performance, while for those films processed in the absence of nanoparticles, the performance order changes because the one cast from an aqueous solution yields higher currents, particularly at low concentrations. This can be understood by the higher hydrophilic character of the film and its random structure compared to the one cast from an organic solvent.

4. CONCLUSIONS

The relationship between the film organization and bioelectrochemical performance is helpful for designing new supramolecular materials and processing strategies leading to electrochemical platforms with optimized properties. To this end, in this work a comprehensive study of the structure/morphology of redox-active nanocomposite polyelectrolyte−surfactant films and its effect on the generation of bioelectrochemical signals through the biocatalytic oxidation of glucose was presented. Using different experimental methods, we demonstrated that the presence of AuNPs has the effect of disrupting the mesoscale organization of the film and, at the same time, plays a role as an "agglomerating agent" for the polyelectrolyte−surfactant complex, maintaining a closer interaction between different supramolecular domains, as reflected by the decrease in the film roughness. The effect of AuNPs is slightly affected by the solvent chosen for the casting process regarding the current generation process. In the absence of AuNP, the casting solvent plays an important role because the one cast from an organic solvent retains its stratified mesostructure, thus reducing the interaction between the redox-active osmium centers and the enzyme. On the other hand, films cast from aqueous solutions exhibit important changes in its mesostructure and morphology that allow a better interaction between the osmium centers and a more suitable environment for the molecular transport of glucose through the film. Finally, this work intended to rationalize the construction of bioelectrochemical interfacial architectures by combining the integration of AuNPs into polyelectrolyte−surfactant complexes using the processing solvent as a new variable to optimize the performance of the nanocomposite film.

■ ASSOCIATED CONTENT

Supporting Information

The Supporting Information is available free of charge on the ACS Publications website at DOI: 10.1021/acsami.6b13456.

Detailed experimental characterization (quartz crystal microbalance, XPS, TGA, and tapping-mode AFM) (PDF)

■ AUTHOR INFORMATION

Corresponding Authors

*E-mail: battagli@qi.fcen.uba.ar.

*E-mail: azzaroni@inifta.unlp.edu.ar. Web: https://softmatter.quimica.unlp.edu.ar. Web: https://www.facebook.com/SoftMatterLaboratory/.

ORCID

Omar Azzaroni: 0000-0002-5098-0612

Notes

The authors declare no competing financial interest.

■ ACKNOWLEDGMENTS

The authors acknowledge financial support from ANPCyT (Grants PICT 2010-2554 and PICT-2013-0905), Fundación Petruzza, Consejo Nacional de Investigaciones Científicas y Técnicas (CONICET; Grant PIP 0370), and the Austrian Institute of Technology GmbH (AIT−CONICET Partner Lab: "Exploratory Research for Advanced Technologies in Supramolecular Materials Science", Exp. 4947/11, Res. No. 3911, 28-12-2011). O.A. and M.C. gratefully acknowledge the LNLS (Campinas, Brazil) for financial support and for granting access to synchrotron facilities (XRD2-13391, XRD2-11639, XRD2-14358, and SXS-11642). M.L.C., M.C., F.B., and O.A. are CONICET fellows.

■ REFERENCES

(1) Ghosh, S.; Maiyalagan, T.; Basu, R. N. Nanostructured Conducting Polymers for Energy Applications: Towards a Sustainable Platform. *Nanoscale* **2016**, *8*, 6921−6947.

(2) Son, E. J.; Kim, J. H.; Kim, K.; Park, C. B. Quinone and Its Derivatives for Energy Harvesting and Storage Materials. *J. Mater. Chem. A* **2016**, *4*, 11179−11202.

(3) Choi, S. Microscale Microbial Fuel Cells: Advances and Challenges. *Biosens. Bioelectron.* **2015**, *69*, 8−25.

(4) Ma, J.; Sahai, Y. Chitosan Biopolymer for Fuel Cell Applications. *Carbohydr. Polym.* **2013**, *92*, 955−975.

(5) Liang, Y.; Li, Y.; Wang, H.; Dai, H. Strongly Coupled Inorganic/Nanocarbon Hybrid Materials for Advanced Electrocatalysis. *J. Am. Chem. Soc.* **2013**, *135*, 2013−2036.

(6) Liu, J.; Liu, Z.; Barrow, C. J.; Yang, W. Molecularly Engineered Graphene Surfaces for Sensing Applications: A Review. *Anal. Chim. Acta* **2015**, *859*, 1−19.

(7) Katsounaros, I.; Cherevko, S.; Zeradjanin, A. R.; Mayrhofer, K. J. J. Oxygen Electrochemistry as a Cornerstone for Sustainable Energy Conversion. *Angew. Chem., Int. Ed.* **2014**, *53*, 102−121.

(8) Coutanceau, C.; Brimaud, S.; Lamy, C.; Léger, J. M.; Dubau, L.; Rousseau, S.; Vigier, F. Review of Different Methods for Developing Nanoelectrocatalysts for the Oxidation of Organic Compounds. *Electrochim. Acta* **2008**, *53*, 6865−6880.

(9) Feifel, S. C.; Kapp, A.; Ludwig, R.; Lisdat, F. Nanobiomolecular Multiprotein Clusters on Electrodes for the Formation of a Switchable

Cascadic Reaction Scheme. *Angew. Chem., Int. Ed.* **2014**, *53*, 5676−5679.
(10) Zayats, M.; Willner, B.; Willner, I. Design of Amperometric Biosensors and Biofuel Cells by the Reconstitution of Electrically Contacted Enzyme Electrodes. *Electroanalysis* **2008**, *20*, 583−601.
(11) Leech, D.; Kavanagh, P.; Schuhmann, W. Enzymatic Fuel Cells: Recent Progress. *Electrochim. Acta* **2012**, *84*, 223−234.
(12) Suginta, W.; Khunkaewla, P.; Schulte, A. Electrochemical Biosensor Applications of Polysaccharides Chitin and Chitosan. *Chem. Rev.* **2013**, *113*, 5458−5479.
(13) Li, J.; Yuan, R.; Chai, Y.; Che, X.; Li, W. Construction of an Amperometric Glucose Biosensor Based on the Immobilization of Glucose Oxidase onto Electrodeposited Pt Nanoparticles-Chitosan Composite Film. *Bioprocess Biosyst. Eng.* **2012**, *35*, 1089−1095.
(14) Scognamiglio, V. Nanotechnology in Glucose Monitoring: Advances and Challenges in the Last 10 Years. *Biosens. Bioelectron.* **2013**, *47*, 12−25.
(15) Ko, S.; Park, T. J.; Kim, H. S.; Kim, J. H.; Cho, Y. J. Directed Self-Assembly of Gold Binding Polypeptide-Protein a Fusion Proteins for Development of Gold Nanoparticle-Based SPR Immunosensors. *Biosens. Bioelectron.* **2009**, *24*, 2592−2597.
(16) Wang, H.; Wu, J.; Li, J.; Ding, Y.; Shen, G.; Yu, R. Nanogold Particle-Enhanced Oriented Adsorption of Antibody Fragments for Immunosensing Platforms. *Biosens. Bioelectron.* **2005**, *20*, 2210−2217.
(17) Katz, E.; Willner, I. Integrated Nanoparticle−Biomolecule Hybrid Systems: Synthesis, Properties, and Applications. *Angew. Chem., Int. Ed.* **2004**, *43*, 6042−6108.
(18) Willner, I.; Willner, B. Functional Nanoparticle Architectures for Sensoric, Optoelectronic, and Bioelectronic Applications. *Pure Appl. Chem.* **2002**, *74*, 1773−1783.
(19) Tel-Vered, R.; Kahn, J. S.; Willner, I. Layered Metal Nanoparticle Structures on Electrodes for Sensing, Switchable Controlled Uptake/Release, and Photo-Electrochemical Applications. *Small* **2016**, *12*, 51−75.
(20) Yehezkeli, O.; Tel-Vered, R.; Raichlin, S.; Willner, I. Nano-Engineered Flavin-Dependent Glucose Dehydrogenase/Gold Nanoparticle-Modified Electrodes for Glucose Sensing and Biofuel Cell Applications. *ACS Nano* **2011**, *5*, 2385−2391.
(21) Chazalviel, J. N.; Allongue, P. On the Origin of the Efficient Nanoparticle Mediated Electron Transfer across a Self-Assembled Monolayer. *J. Am. Chem. Soc.* **2011**, *133*, 762−764.
(22) Barfidokht, A.; Ciampi, S.; Luais, E.; Darwish, N.; Gooding, J. J. Distance-Dependent Electron Transfer at Passivated Electrodes Decorated by Gold Nanoparticles. *Anal. Chem.* **2013**, *85*, 1073−1080.
(23) Udeh, C. U.; Fey, N.; Faul, C. F. J. Functional Block-Like Structures from Electroactive Tetra(Aniline) Oligomers. *J. Mater. Chem.* **2011**, *21*, 18137−18153.
(24) Ahmed, R.; Hsiao, M.-S.; Matsuura, Y.; Houbenov, N.; Faul, C. F. J.; Manners, I. Redox-Active Mesomorphic Complexes from the Ionic Self-Assembly of Cationic Polyferrocenylsilane Polyelectrolytes and Anionic Surfactants. *Soft Matter* **2011**, *7*, 10462−10471.
(25) Wei, Z.; Faul, C. F. J. Aniline Oligomers − Architecture, Function and New Opportunities for Nanostructured Materials. *Macromol. Rapid Commun.* **2008**, *29*, 280−292.
(26) Wei, Z.; Laitinen, T.; Smarsly, B.; Ikkala, O.; Faul, C. F. J. Self-Assembly and Electrical Conductivity Transitions in Conjugated Oligoaniline−Surfactant Complexes. *Angew. Chem., Int. Ed.* **2005**, *44*, 751−756.
(27) Cheng, Z. Y.; Ren, B. Y.; Chang, X. Y.; Liu, R.; Tong, Z. Novel Redox-Active Ionic Thermotropic Liquid Crystalline Complexes of Polyelectrolyte and Ferrocenyl Surfactants. *Chin. Chem. Lett.* **2012**, *23*, 619−622.
(28) Cheng, Z.; Ren, B.; Zhao, D.; Liu, X.; Tong, Z. Novel Thermotropic Liquid Crystalline and Redox-Active Complexes of Ionically Self-Assembled Poly(Ferrocenylsilane) and Dendritic Amphiphiles. *Macromolecules* **2009**, *42*, 2762−2766.
(29) Cheng, Z.; Ren, B.; Gao, M.; Liu, X.; Tong, Z. Ionic Self-Assembled Redox-Active Polyelectrolyte-Ferrocenyl Surfactant Complexes: Mesomorphous Structure and Electrochemical Behavior. *Macromolecules* **2007**, *40*, 7638−7643.
(30) Faul, C. F. J. Liquid-Crystalline Materials by the Ionic Self-Assembly Route. *Mol. Cryst. Liq. Cryst.* **2006**, *450*, 255−265.
(31) Faul, C. F. J.; Antonietti, M. Ionic Self-Assembly: Facile Synthesis of Supramolecular Materials. *Adv. Mater.* **2003**, *15*, 673−683.
(32) Faul, C. F. J. Ionic Self-Assembly for Functional Hierarchical Nanostructured Materials. *Acc. Chem. Res.* **2014**, *47*, 3428−3438.
(33) Thünemann, A. F. Polyelectrolyte-Surfactant Complexes. Synthesis, Structure and Materials Aspects. *Prog. Polym. Sci.* **2002**, *27*, 1473−1572.
(34) Macknight, W. J.; Ponomarenko, E. A.; Tirrell, D. A. Self-Assembled Polyelectrolyte - Surfactant Complexes in Nonaqueous Solvents and in the Solid State. *Acc. Chem. Res.* **1998**, *31*, 781−788.
(35) Cortez, M. L.; Ceolín, M.; Azzaroni, O.; Battaglini, F. Electrochemical Sensing Platform Based on Polyelectrolyte-Surfactant Supramolecular Assemblies Incorporating Carbon Nanotubes. *Anal. Chem.* **2011**, *83*, 8011−8018.
(36) Cortez, M. L.; González, G. A.; Battaglini, F. An Electroactive Versatile Matrix for the Construction of Sensors. *Electroanalysis* **2011**, *23*, 156−160.
(37) Cortez, M. L.; González, G. A.; Ceolín, M.; Azzaroni, O.; Battaglini, F. Self-Assembled Redox Polyelectrolyte-Surfactant Complexes: Nanostructure and Electron Transfer Characteristics of Supramolecular Films with Built-in Electroactive Chemical Functions. *Electrochim. Acta* **2014**, *118*, 124−129.
(38) Cortez, M. L.; Marmisollé, W.; Pallarola, D.; Pietrasanta, L. I.; Murgida, D. H.; Ceolín, M.; Azzaroni, O.; Battaglini, F. Effect of Gold Nanoparticles on the Structure and Electron-Transfer Characteristics of Glucose Oxidase Redox Polyelectrolyte-Surfactant Complexes. *Chem. - Eur. J.* **2014**, *20*, 13366−13374.
(39) Calvo, E. J.; Battaglini, F.; Danilowicz, C.; Wolosiuk, A.; Otero, M. Layer-by-Layer Electrostatic Deposition of Biomolecules on Surfaces for Molecular Recognition, Redox Mediation and Signal Generation. *Faraday Discuss.* **2000**, *116*, 47−65.
(40) Scodeller, P.; Williams, F. J.; Calvo, E. J. Xps Analysis of Enzyme and Mediator at the Surface of a Layer-by-Layer Self-Assembled Wired Enzyme Electrode. *Anal. Chem.* **2014**, *86*, 12180−12184.
(41) Dronov, R.; Kurth, D. G.; Möhwald, H.; Spricigo, R.; Leimkühler, S.; Wollenberger, U.; Rajagopalan, K. V.; Scheller, F. W.; Lisdat, F. Layer-by-Layer Arrangement by Protein-Protein Interaction of Sulfite Oxidase and Cytochrome C Catalyzing Oxidation of Sulfite. *J. Am. Chem. Soc.* **2008**, *130*, 1122−1123.
(42) Godman, N. P.; DeLuca, J. L.; McCollum, S. R.; Schmidtke, D. W.; Glatzhofer, D. T. Electrochemical Characterization of Layer-by-Layer Assembled Ferrocene-Modified Linear Poly(Ethylenimine)/Enzyme Bioanodes for Glucose Sensor and Biofuel Cell Applications. *Langmuir* **2016**, *32*, 3541−3551.
(43) Kim, J. H.; Hong, S.-G.; Sun, H. J.; Ha, S.; Kim, J. Precipitated and Chemically-Crosslinked Laccase over Polyaniline Nanofiber for High Performance Phenol Sensing. *Chemosphere* **2016**, *143*, 142−147.
(44) Guerrieri, A.; Ciriello, R.; Cataldi, T. R. I. A Novel Amperometric Biosensor Based on a Co-Crosslinked L-Lysine-A-Oxidase/Overoxidized Polypyrrole Bilayer for the Highly Selective Determination of L-Lysine. *Anal. Chim. Acta* **2013**, *795*, 52−59.
(45) Cortez, M. L.; Ceolín, M.; Azzaroni, O.; Battaglini, F. Formation of Redox-Active Self-Assembled Polyelectrolyte-Surfactant Complexes Integrating Glucose Oxidase on Electrodes: Influence of the Self-Assembly Solvent on the Signal Generation. *Bioelectrochemistry* **2015**, *105*, 117−122.
(46) Palermo, V.; Morelli, S.; Simpson, C.; Mullen, K.; Samori, P. Self-Organized Nanofibers from a Giant Nanographene: Effect of Solvent and Deposition Method. *J. Mater. Chem.* **2006**, *16*, 266−271.
(47) Lena, S.; Brancolini, G.; Gottarelli, G.; Mariani, P.; Masiero, S.; Venturini, A.; Palermo, V.; Pandoli, O.; Pieraccini, S.; Samorì, P.; Spada, G. P. Self-Assembly of an Alkylated Guanosine Derivative into Ordered Supramolecular Nanoribbons in Solution and on Solid Surfaces. *Chem. - Eur. J.* **2007**, *13*, 3757−3764.

DOI: 10.1021/acsami.6b13456
ACS Appl. Mater. Interfaces 2017, 9, 1119−1128

(48) De Luca, G.; Pisula, W.; Credgington, D.; Treossi, E.; Fenwick, O.; Lazzerini, G. M.; Dabirian, R.; Orgiu, E.; Liscio, A.; Palermo, V.; Müllen, K.; Cacialli, F.; Samorì, P. Non-Conventional Processing and Post-Processing Methods for the Nanostructuring of Conjugated Materials for Organic Electronics. *Adv. Funct. Mater.* **2011**, *21*, 1279−1295.
(49) Danilowicz, C.; Corton, E.; Battaglini, F. Osmium Complexes Bearing Functional Groups: Building Blocks for Integrated Chemical Systems. *J. Electroanal. Chem.* **1998**, *445*, 89−94.
(50) Kiely, C. J.; Fink, J.; Brust, M.; Bethell, D.; Schiffrin, D. J. Spontaneous Ordering of Bimodal Ensembles of Nanoscopic Gold Clusters. *Nature* **1998**, *396*, 444−446.
(51) Sader, J. E.; Sanelli, J. A.; Adamson, B. D.; Monty, J. P.; Wei, X.; Crawford, S. A.; Friend, J. R.; Marusic, I.; Mulvaney, P.; Bieske, E. J. Spring Constant Calibration of Atomic Force Microscope Cantilevers of Arbitrary Shape. *Rev. Sci. Instrum.* **2012**, *83*, 103705.
(52) Thünemann, A. F.; Müller, M.; Dautzenberg, H.; Joanny, J. F.; Löwen, H. Polyelectrolyte Complexes. *Adv. Polym. Sci.* **2004**, *166*, 113−171.
(53) Thünemann, A. F.; General, S. Nanoparticles of a Polyelectrolyte-Fatty Acid Complex: Carriers for Q10 and Triiodothyronine. *J. Controlled Release* **2001**, *75*, 237−247.
(54) Antonietti, M.; Conrad, J.; Thünemann, A. Polyelectrolyte-Surfactant Complexes: A New Type of Solid, Mesomorphous Material. *Macromolecules* **1994**, *27*, 6007−6011.
(55) Bolze, J.; Takahasi, M.; Mizuki, J.; Baumgart, T.; Knoll, W. X-Ray Reflectivity and Diffraction Studies on Lipid and Lipopolymer Langmuir-Blodgett Films under Controlled Humidity. *J. Am. Chem. Soc.* **2002**, *124*, 9412−9421.
(56) Cortez, M. L.; Cukierman, A. L.; Battaglini, F. Surfactant Presence in a Multilayer Polyelectrolyte-Enzyme System Improves Its Catalytic Response. *Electrochem. Commun.* **2009**, *11*, 990−993.
(57) Holly, F. J. Novel Methods of Studying Polymer Surfaces by Employing Contact Angle Goniometry. In *Physicochemical Aspects of Polymer Surfaces*; Mittal, K. L., Ed.; Plenum Press: New York, 1983; Vol. *1*, pp 141−154.
(58) Chen, W.; McCarthy, T. J. Layer-by-Layer Deposition: A Tool for Polymer Surface Modification. *Macromolecules* **1997**, *30*, 78−86.

DOI: 10.1021/acsami.6b13456
ACS Appl. Mater. Interfaces 2017, 9, 1119−1128